Fuel 212 (2018) 332–346

Contents lists available at ScienceDirect

Fuel

journal homepage: www.elsevier.com/locate/fuel

Full Length Article

An experimental and numerical study on diesel injection split of a natural gas/diesel dual-fuel engine at a low engine load

Amin Yousefi[a], Hongsheng Guo[b,*], Madjid Birouk[a,*]

[a] Department of Mechanical Engineering, University of Manitoba, Winnipeg, Manitoba R3T 5V6, Canada
[b] Energy, Mining and Environment Portfolio, National Research Council Canada, 1200 Montreal Road, Ottawa, Ontario K1A 0R6, Canada

ARTICLE INFO

Keywords:
Dual-fuel combustion
Conventional single diesel injection timing
Split injection mode

ABSTRACT

Natural gas/diesel dual-fuel combustion is currently one of the most promising LTC strategies for the next generation of heavy-duty engines. While this concept is not new and it has been deliberated lengthily in the past two decades, several uncertainties still exist. A major shortcoming of this concept is associated with its low thermal efficiency and high level of unburned methane and CO emissions under low engine load conditions. The present paper reports an experimental and numerical study on the effect of different injection strategies (single and two pulses injection of pilot diesel fuel) on the combustion performance and emissions of a heavy duty natural gas/diesel dual-fuel engine at 25% engine load. The results of single diesel injection mode showed that advancing diesel injection timing from 10 to 30 °BTDC reduced unburned methane and CO emissions by 62% and 61% and increased thermal efficiency by 6%; however, NO_x emissions increased by 74%. In order to achieve NO_x – CH_4 and NO_x – CO trade-off and increased thermal efficiency at low load conditions, the effect of split injection strategy was experimentally and numerically examined. The results of split injection mode revealed that split injection strategy considerably increases the in-cylinder peak pressure compared to that of single injection (10 °BTDC). The results showed also that the heat release produced by the first injection of diesel fuel considerably increased the in-cylinder charge temperature before the start of the second injection. The flame zone of the split injection mode is markedly higher than that of the single injection due to larger heat release produced during the first injection which promotes the combustion of the second one. When the first injection timing is close to the second injection timing, the MPRR of split injection mode is higher than that of single injection (10 °BTDC). However, further advancing of the first injection timing continuously decreased the MPRR. OH radical analysis showed that for advanced first injection timings (38–50 °BTDC), the overall growth rate of OH radical becomes slower and its distribution is narrower as indicated by the wider non-reactive blue zones compared with those observed at a late first injection timing in the initial stages of combustion. However, OH radicals gradually grow during last stages of combustion in the expansion stroke, indicating that a more pre-mixed combustion takes place in these cases. For very advanced first injection timing of 55 °BTDC, the OH distribution is similar to that of the single injection mode with lower OH intensity at initial stages of combustion and they barely grow during the late expansion stroke. At this condition, the ignition of premixed mixture is mainly controlled by the second diesel fuel injection. The trade-off between NO_x – CH_4 and NO_x – CO is achieved when applying split injection. Compared to single injection (10 °BTDC), the first injection timing of 50 °BTDC decreased unburned methane and CO emissions by 60% and 63%, respectively, and increased the thermal efficiency by 8.9%. However, NO_x emissions were maintained at the same level as single injection mode (10 °BTDC).

Abbreviations: ADIT, After Diesel Injection Timing; AMDIT, After Main Diesel Injection Timing; ASOC, After Start of Combustion; ASOI, After Start of Injection; BMEP, Break Mean Effective Pressure; BTDC, Before Top Dead Center; BTE, Break Thermal Efficiency; CA, Crank Angle; CFD, Computational Fluid Dynamic; CI, Compression Ignition; CO, Carbon monoxide; DIT, Diesel Injection Timing; EGR, Exhaust Gas Recirculation; EOI, End of Injection; EVO, Exhaust Valve Opening; HCCI, Homogeneous Charge Compression Ignition; HRR, Heat Release Rate; ITE, Indicated Thermal Efficiency; LHV, Lower Heating Value; LTC, Low Temperature Combustion; MPRR, Maximum Pressure Rise Rate; NO_x, Nitrogen Oxides; SOC, Start of Combustion; SOI, Start of Injection; TDC, Top Dead Center; THC, Total Hydrocarbon; UHC, Unburned Hydrocarbon; VCR, Variable Compression Ratio

* Corresponding authors.
E-mail addresses: Hongsheng.Guo@nrc-cnrc.gc.ca (H. Guo), madjid.birouk@umanitoba.ca (M. Birouk).

http://dx.doi.org/10.1016/j.fuel.2017.10.053
Received 1 August 2017; Received in revised form 24 September 2017; Accepted 10 October 2017
Available online 20 October 2017
0016-2361/

1. Introduction

The usage of petroleum as an energy source is expected to decrease due to limited global oil reserves, its negative impact on the environment, and stringent emissions regulations. This will affect compression ignition (CI) diesel engines which play significant role in transportation and power generation, where there is a need for cleaner, more economical, and reliable alternative fuels. Conventional diesel engines also suffer from high soot emissions due to the over-rich regions in the core area of the fuel spray and high nitrogen oxides (NO_x) emissions as a result of high flame temperature of the stoichiometric fuel-air mixture at the periphery of the fuel spray. In order to reduce both soot and NO_x emissions, fuel-rich and high temperature stoichiometric regions should be avoided simultaneously [1]. An effective approach is to employ low temperature combustion (LTC) strategies which are featured by improved fuel atomization, mixture preparation, lower local equivalence ratios, reduced local temperature, and alternative fuels [2]. Homogeneous charge compression ignition (HCCI) combustion is one of such strategies characterized by early fuel injection, which promotes fuel premixed charge, long ignition delay, and short combustion duration. Ignition timing is kinetically controlled and therefore decoupled from the timing of the fuel injection event [3,4]. However, the lack of direct control of ignition timing and combustion phasing, higher unburned hydrocarbon (UHC) and carbon monoxide (CO) emissions, as well as knock and misfiring under transient conditions, are the major drawbacks of HCCI combustion engines [5–8]. In contrast, some slightly more heterogeneous combustion strategies have been developed to overcome the majority of the aforementioned challenges. For example, the charge distribution is more heterogeneous than HCCI combustion as it consists of lean and rich regions at the time of ignition. Moreover, ignition timing is closely coupled to the fuel injection timing, though chemical kinetics still play an important role [3].

Natural gas/diesel dual-fuel combustion is one of these LTC strategies which allow a higher degree of combustion phasing control while maintaining low soot and NO_x emissions. In a dual-fuel engine, the primary method of fuel delivery is the port injection of natural gas which creates well-mixed charge of premixed fuel-air, while a small amount of diesel fuel is directly injected into the cylinder as the ignition source. Natural gas/diesel dual-fuel combustion tends to retain most and even surpasses occasionally the positive features of conventional diesel engines, and producing comparable power output and efficiency at different engine loads [9–11]. In addition, natural gas/diesel dual-fuel mode has attracted much interests due to other advantages, such as simple modification from a diesel engine and the flexibility in switching back to fully diesel mode [12]. Moreover, this combustion concept relies on natural gas as the major energy source, which yields lower carbon dioxide (CO_2) emissions due to the higher hydrogen to carbon ratio. However, there still exist some issues that are limiting the application of natural gas/diesel dual-fuel engines. One of these issues is the low thermal efficiency and higher unburned methane and CO emissions at low engine load conditions. At low load conditions, a natural gas/diesel dual-fuel engine is fed with a very lean air-fuel mixture which is difficult to ignite and burn, leading to significant levels of unburned methane and CO emissions. This is because, at very lean air-methane mixtures, portions of the charge which resides far away from diesel fuel spray escape the combustion process [13–15]. Numerous studies have addressed these issues by examining the effect of combustion boundaries, such as diesel injection timing and pressure [16–20], natural gas energy fraction [20–24], variable compression ratio (VCR) [25–27], natural gas injection timing [20,28], and the use of exhaust gas recirculation (EGR) [29,30]. Among these strategies, diesel injection timing change is of great interest and usually regarded as a critical factor which has influence on the combustion performance and emissions characteristics.

Various researchers have examined the effect of conventional diesel injection timing (i.e., 5–30 °before top dead center (BTDC)) on thermal efficiency and unburned methane and CO emissions of natural gas/diesel dual-fuel mode at low conditions [10,14,17,31–34]. For instance, Zhang et al. [34] examined the effect of diesel injection timing (DIT) sweep (DIT = 7–25 °BTDC with 2 °crank angle (CA) increment) on combustion performance and emissions of natural gas/diesel dual-fuel mode and found that total hydrocarbon (THC) and CO emissions reduced with advancing diesel injection timing. On the other hand, they noted increased NO_x emissions with advanced diesel injection timing due to higher in-cylinder temperature. Yang et al. [14] investigated various diesel injection timings (DIT = 5–29 °BTDC with 4°CA increment) in a natural gas/diesel dual-fuel engine at a low engine load. They reported that advancing diesel injection timing from 5 to 29 °BTDC significantly increased break thermal efficiency (BTE). Moreover, they observed that, with advancing diesel injection timing, THC and CO emissions notably decreased due to the relatively higher combustion rate and greater utilization of premixed natural gas at earlier injection timings. Similar to the findings in [34], NO_x emission was observed to significantly increase with advancing diesel injection timing in [14]. Wang et al. [33] also observed that advancing diesel injection timing from −5 to 22.5 °BTDC drastically increased NO_x emissions, while decreased THC emissions.

Based on the briefly reviewed literature above, it is revealed that advancing diesel injection timing in the range of conventional diesel injection timing (i.e., 5–30 °BTDC) improved thermal efficiency as well as unburned methane and CO emissions but generated higher NO_x emissions. To address this issue, various single pulse conventional diesel injection timings (10–30 °BTDC with 4°CA increment) are experimentally and numerically examined in the present paper using a natural gas/diesel dual-fuel combustion with 75% natural gas energy fraction under 25% engine load (break mean effective pressure (BMEP) = 4.05 bar). Afterwards, the effect of diesel injection split (two pulses injection) as a feasible method to decrease both NO_x and unburned methane emissions and increase thermal efficiency is examined under the same engine load condition. In particular, the effect of first pulse injection timing (28–55 °BTDC) with fixed split injection ratio of 60% and second pulse injection timing of 10 °BTDC on combustion performance and emissions of natural gas/diesel dual-fuel engine is investigated. This provides useful information for the optimization of diesel injection strategy for natural gas/diesel dual-fuel combustion at low load engine conditions.

2. Experiments

2.1. Test engine

The engine used in this investigation is a modified single-cylinder version of Caterpillar's 3400-series heavy-duty engine. More details about the experimental setup and engine configuration can be found elsewhere [35]. Table 1 lists the specifics of the engine and Fig. 1 depicts the schematic diagram of test setup.

Natural gas was injected into the intake port by a fuel injection manifold. Diesel fuel was directly injected into the cylinder using a prototype common-rail fuel injector system. The start of injection and injection pulse width for both diesel and natural gas were controlled by a driven system provided by National Instruments (model PXI-1031chassis, 8184 embedded controller, and 7813 R RIO card connected to cRIO-9151 expansion chassis) and LabVIEW-based software (Drivven Inc., Stand-Alone Direct Injector Drive System). The flow rates of diesel and natural gas were measured by two Bronkhorst mass flowmeters, respectively, and the flow rate of air was measured by a turbine mass flowmeter.

2.2. Fuels and their supply systems

Diesel fuel used in this study was a Canadian ultra-low-sulfur diesel (ULSD), and the natural gas used in this research was supplied by

Table 1
Engine specifications.

Engine type	Single cylinder-caterpillar 3400 heavy duty engine
Bore × Stroke	137.2 mm × 165.1 mm
Conn. rod length	261.62 mm
Displacement vol.	2.44 L
Compression ratio	16.25
Diesel fuel injector	Common rail injector
Injector tip length	1.51 mm
Number of nozzle hole × diameter	6 × 0.23 mm
Natural gas injection timing	−355 °ATDC
Inlet valve opening (IVO)	−358.3 °ATDC
Inlet valve closing (IVC)	−169.7 °ATDC
Exhaust valve opening (EVO)	145.3 °ATDC
Exhaust valve closing (EVC)	348.3 °ATDC

Enbridge Inc. Table 2 gives the properties of both diesel and natural gas used in this study. During the experiment, natural gas energy fraction, which is defined as the energy of natural gas divided by total energy of natural gas and diesel fuel, was kept constant at 75%.

2.3. Test procedure and conditions

The experiments were conducted at an engine speed of 910 rpm and a brake mean effective pressure (BMEP) of 4.05 bar, which corresponded to 25% engine load. The intake temperature was kept constant at 40 °C during the experiments. The intake and exhaust manifold pressures were kept at 1.05 and 1.20 bar, respectively. The diesel injector rail pressure was 525 bar. EGR was not used in this study. During the tests, a sweep of diesel injection timing for both single injection and split injection modes was conducted.

2.4. Diesel injection strategies

The injection strategies employed in this study consisted of a single and two-pulse injections. For the two-pulse injection strategy, the first pulse injection timing was swept from 55 to 28 °BTDC, while the second pulse injection timing was kept constant at 10 °BTDC. The split ratio, which is defined as the mass of the diesel fuel injected in the first pulse over the total mass of the injected diesel fuel, was set at 60%. Table 3 shows details of the diesel injection strategies tested in the experiments.

Table 2
Fuel properties.

Fuel type	Natural gas	Diesel
Density (kg/m^3)		814.8
Cetane number	–	44
LHV (MJ/kg)	48.4	44.64
Viscosity (cSt 40 °C)		1.483
H/C ratio	–	1.90
Component (% Vol)	Methane: 96.186	
	Ethane: 1.741	
	Propane: 0.100	
	Hexanes: 0.012	
	Nitrogen: 1.372	
	Carbon dioxide: 0.589	

3. Numerical models

3.1. Flow and combustion modelling

Details of the model were reported in [36] and thus only a brief description is given here. Numerical simulations were performed using AVL-FIRE v2014 software coupled with CHEMKIN solver for flow and chemistry calculations. Both flow and combustion were modelled by solving the complete set of Navier-Stokes equations. CHEMKIN package was used to acquire reactions rates and thermal and transport properties of species. A reactions mechanism, consisting of 42 species and 168 reactions, developed at Chalmers University [37] and validated at engine relevant conditions by Aggarwal [38] was used in the calculation. In this chemical mechanism, n-heptane was used to represent diesel, and methane was used to represent natural gas. The Heywood original NO_x mechanism was used in this study to account for thermal and prompt NO_x formation [39]. To reduce the computational cost, soot emissions were not considered in the simulation, since soot prediction needs a more complex reaction mechanism. However, our experimental measurements showed that soot emissions for dual-fuel engine are very low [40]. Therefore, neglecting soot in the simulation should have insignificant effect on the results of other parameters. The ''Kong-Reitz'' combustion model was used in the simulation. It assumes that the reaction rate of each species is determined by the kinetic process and the relative magnitude of mixing and reaction, which can be characterized by a local Damköhler number defined as the ratio of flow mixing to kinetic time scale [41]. Renormalization group (RNG) k-ε turbulence model, Reynolds Averaged Navier-Stokes (RANS), and pressure implicit

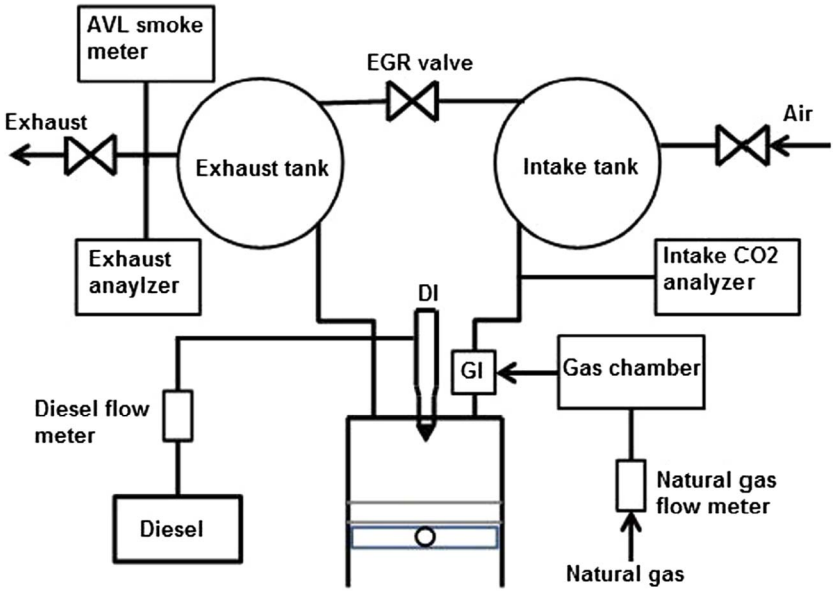

Fig. 1. Schematic diagram of the experimental setup [35].

Table 3
Experimental test cases – single and split injection strategies under 75% natural gas energy fraction and 25% engine load.

Injection strategy	Air flow (kg/h)	Diesel flow (kg/h)	NG flow (kg/h)	SOI (°BTDC)	EOI (°BTDC)		
Single injection	66.93	0.5238	1.470	10	3.57	–	–
	67.21	0.4948	1.389	14	7.71		
	67.57	0.4710	1.306	18	11.81		
	67.45	0.4503	1.259	22	15.89		
	67.08	0.4370	1.237	26	19.95		
	66.7053	0.4552	1.2345	30	23.86		
				SOI1 (°BTDC)	EOI1 (°BTDC)	SOI2 (°BTDC)	EOI2 (°BTDC)
Split injection (60/40%)	63.89	0.4346	1.207	28	22.53	10	6.35
	63.81	0.4266	1.197	30	24.55		6.37
	63.91	0.4271	1.186	34	28.56		6.38
	63.03	0.4212	1.181	38	32.65		6.43
	64.15	0.4168	1.178	42	36.57		6.38
	64.14	0.4206	1.152	46	40.47		6.31
	64.16	0.4131	1.146	50	44.48		6.32
	64.02	0.4294	1.178	55	49.51		6.34

with splitting of operators (PISO) algorithm were used to simulate the transient turbulent flow in the combustion chamber [42]. In the present study, the flow behaviour near the cylinder wall and the heat transfer between the working fluid and the cylinder wall were modeled using the Hybrid Wall Treatment and Standard Wall Function models [39].

3.2. Spray modelling

The break-up process of diesel liquid fuel was simulated using WAVE model based on the physical properties (for the spray and mixing process) of diesel fuel [43]. In this model, the growth of an initial perturbation on the liquid surface is linked to its wavelength and other physical and dynamic parameters of the injected fuel and the in-cylinder gas. There exist two break-up regimes, one for high velocity Kevin-Helmholtz (KH) type and the other for low velocity Rayleigh-Taylor (RT) type break-up [44]. For the first case, the size of droplets is set equal to the wavelength of the fastest growing or most probable unstable surface wave. Rayleigh type break-up produces droplets that are larger than the original parent drops. This regime is not important for high pressure injection systems. The use of WAVE model in the present study, which was developed for KH instabilities, is an appropriate approach for high pressure injection system [43]. Primary parcels (blobs) are injected with a diameter similar to the nozzle orifice and a velocity which is a function of the injected mass flow rate. Particles passing through the flow interact with turbulent eddies. Such interaction results in deflecting particles by the instantaneous velocity of turbulent eddies and particles inertia. This additional turbulence effect on the spray particles could not be resolved by the flow field and consequently the O'Rourke turbulent dispersion model was used in the present study [43]. Moreover, Dukowicz model [45] was used for the heat-up and evaporation of droplets. It assumes that droplets evaporate in a non-condensable gas environment. Therefore, it uses a two-component system in the gas-phase which consists of vapor and non-condensable gas where each component may be composed of a mixture of different species.

3.3. Computational domain and initial conditions

The computational mesh was created by FIRE ESE-Diesel platform. Since the diesel injector has six equally spaced nozzle's orifices, a sector mesh of 60 °was used to model one spray plume to take advantage of the axial symmetry. To ensure mesh independency, an optimized average cell size of 1.5 mm consisting of 28,833 control volumes at the top dead center (TDC) and 76,020 control volumes at the bottom dead center (BDC) was used. Further refinement of the mesh resolution up to 1 mm did not produce any significant improvement in the accuracy of the predictions, while the required computational runtime was 30% longer. The simulation time step was varied in the range from 0.25 to 0.5 crank angle (°CA) based on the temporal gradients of the computed parameters. Computation was performed in series using a 8-core processor and lasted approximately 6 h CPU time. The computational domain at the TDC is shown in Fig. 2. The boundary conditions at the engine head and piston surfaces were defined as impermeable wall boundary conditions. The cylinder geometry was assumed to be symmetric around the cylinder axis, and cyclic boundary conditions were applied to the cutting surfaces as shown in Fig. 2. Simulation was initialized at IVC and terminated prior to EVO. The port fuel injected natural gas was considered to be homogeneously mixed with air at IVC. Table 4 provides the boundary and initial conditions for the numerically simulated cases.

3.4. Test conditions

According to the experimental test cases (Table 3), all test conditions, including engine load (25% load and BMEP = 4.05 bar), speed (910 rpm), natural gas energy fraction (75%), diesel injector rail pressure (525 bar), and intake temperature and pressure (P_{intake} = 1.05 bar, T_{intake} = 313 K, and EGR = 0%) were kept constant during the simulation and only the effect of different diesel injection strategies (i.e., single and double pulse injections) on the combustion performance and emissions of dual-fuel combustion was investigated.

4. Result and discussion

This section first reports the experimental and numerical results of the effect of conventional single injection timings (10–30 °BTDC) on combustion performance and emissions of natural gas/diesel dual-fuel combustion at 25% engine load (BMEP = 4.05 bar). All test conditions, including engine load (25% load and BMEP = 4.05 bar), speed (910 rpm), natural gas energy fraction (75%), diesel injector rail pressure (525 bar), and intake temperature and pressure (P_{intake} = 1.05 bar, T_{intake} = 313 K, and EGR = 0%) were kept constant and only diesel

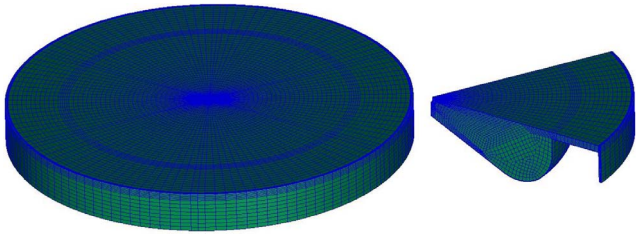

Fig. 2. Computational domain of complete (left) and one-sixth (right) of the combustion chamber at TDC.

Table 4
Initial and boundary conditions.

Boundary conditions	Boundary type/specific condition
Cylinder head	Wall-temperature 400 K
Piston	Mesh movement-temperature 400 K
Segment cut	Periodic inlet/outlet
Liner	Wall-temperature 400 K
Initial conditions	
Pressure at IVC	1.02 bar
Temperature at IVC	360 K
Turb. kin. energy	10 m^2/s^2
Turb. length scale	0.003 m
Turb. diss. Rate	1732 m^2/s^3

injection timing was swept in the range between 10 and 30 °BTDC with an increment of 4 °CA. Then the experimental and numerical results of the effect of split injection (two pulses injection) on combustion performance and emissions of dual-fuel engine are provided. Numerical simulation results including in-cylinder pressure, heat release rate (HRR), thermal efficiency, emissions of NO_x, CO and unburned methane, and spatial and temporal contours of the mean charge temperature and OH radical are provided to help understand the behaviour of natural gas/diesel dual-fuel combustion process at low engine load conditions.

4.1. Single injection

Fig. 3 shows the effect of conventional injection timing (10–30 °BTDC) on the in-cylinder pressure and HRR of natural gas/diesel dual-fuel mode at 25% engine load (BMEP = 4.05 bar). In this study, the measured and calculated HRR was obtained from the average in-cylinder pressure based on the first law of thermodynamics and the ideal gas law. It can be seen that there is a good match between the measured and calculated in-cylinder pressure and HRR profiles, demonstrating the ability of the CFD model along with the adopted reaction

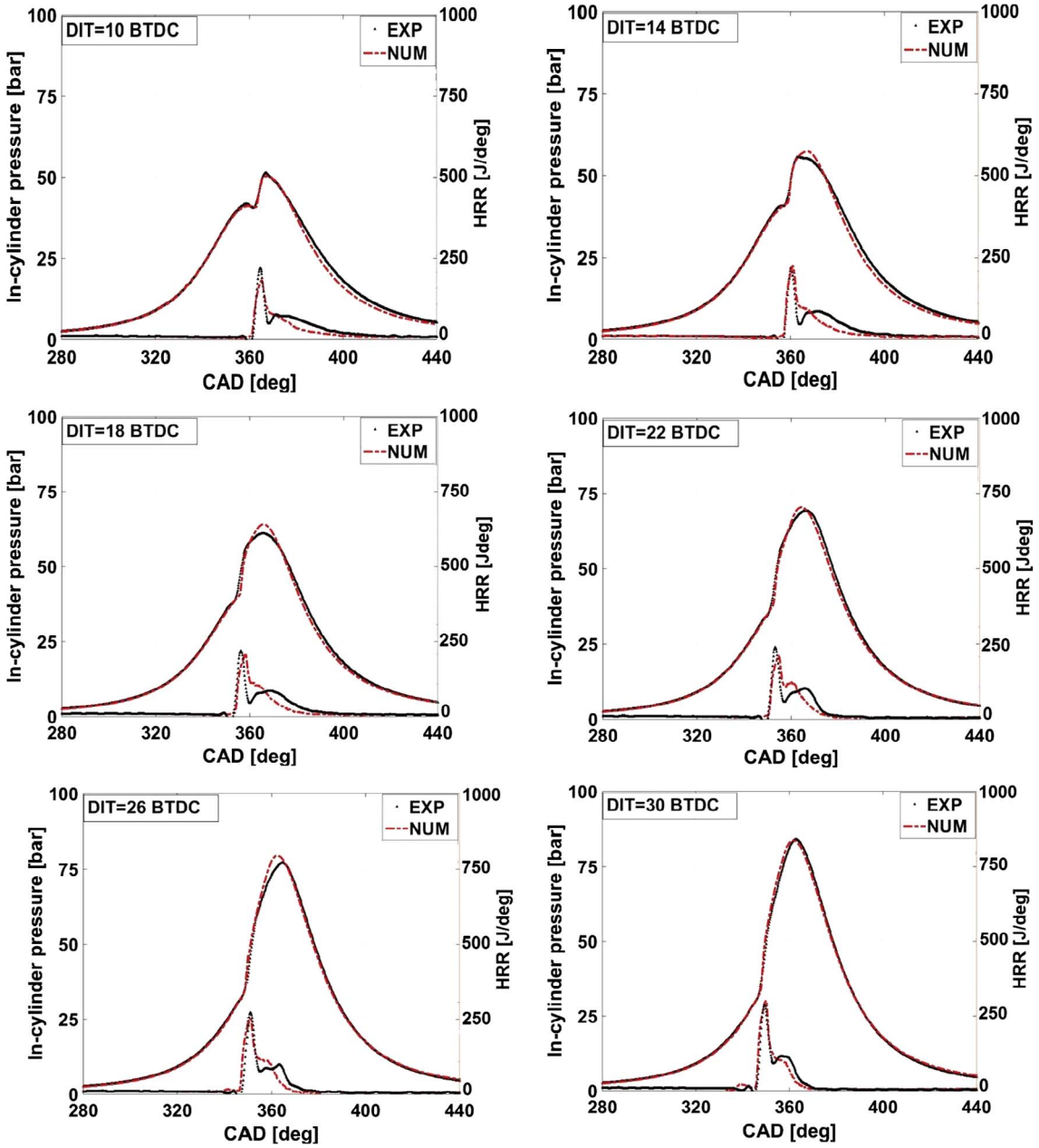

Fig. 3. Comparison of experimental and numerical in-cylinder pressure and HRR of dual-fuel mode with single injection mode under 25% engine load.

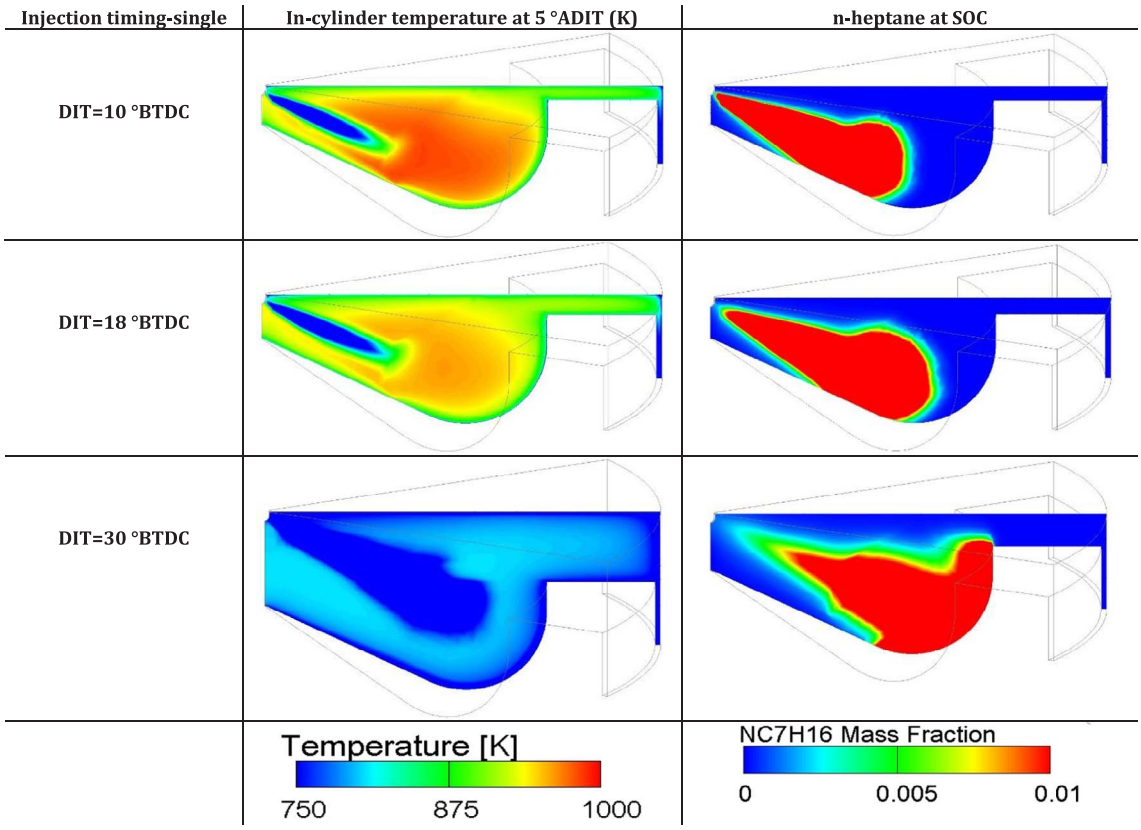

Fig. 4. In-cylinder temperature (at 5 °CA ADIT) and n-heptane (at SOC) contours of dual-fuel mode with single injection under 25% engine load.

mechanism. Advancing the injection timing up to 30 °BTDC increases the maximum in-cylinder pressure and shifts the in-cylinder peak pressure close to the TDC. The in-cylinder temperature during the diesel injection and before start of combustion (SOC) largely affects the premixed mixture formation. Fig. 4 displays the in-cylinder temperature contours at 5°CA after diesel injection timing (ADIT) and n−heptane mass fraction distribution at SOC for three selected diesel injection timings. As shown in this figure, at injection timing of 30 °BTDC the mixing process occurs earlier in the compression stroke and consequently lower temperature is present in the combustion chamber during the diesel injection and before SOC. This leads to a prolonged ignition delay and consequently more premixed mixture (diesel and premixed natural gas-air) is formed during the ignition delay period when advancing the diesel injection timing from 10 to 30 °BTDC (Fig. 4). Earlier injection timing tends to advance the combustion phasing while prolonged ignition delay tends to retard combustion phasing. The effect of advancing diesel injection timing is more significant than that of prolonged ignition delay, leading to the shift of combustion phasing toward TDC and thus higher maximum in-cylinder pressure when advancing diesel injection timing from 10 to 30 °BTDC.

Fig. 5a displays the variation of the indicated thermal efficiency (ITE) as a function of diesel injection timing (single injection) under 25% engine load. Advancing the diesel injection timing from 10 to 30 °BTDC significantly increases the thermal efficiency (6%). This is due to the fact that advancing the diesel injection timing prolongs the ignition delay and thus more premixed natural gas-air and diesel mixture is formed before SOC which leads to larger number and wider space distribution of ignition kernel. As a result, combustion efficiency of natural gas is improved, which can be shown by Fig. 5b and c that show that advancing diesel injection timing from 10 to 30 °BTDC considerably reduces unburned methane and CO emissions, whereas increases NO_x emissions. Simulation results show that unburned methane and CO emissions are reduced by 62% and 61%, respectively. Advancing diesel injection timing enhanced the entrainment of premixed natural gas into the ignition kernels and consequently the combustion process becomes faster and complete, which is the main reason of the reduction in methane and CO emissions. However, NO_x emissions are increased by 61.3% when diesel injection timing is advanced from 10 to 30 °BTDC. This is due to the fact that the local gas temperature becomes higher and more homogeneous mixture is formed in the cylinder as diesel injection timing advances. Therefore, natural gas/diesel dual-fuel engine experiences improved thermal efficiency and unburned methane and CO emissions but at the expense of higher NO_x emissions when diesel injection is advanced from 10 to 30 °BTDC. This is not in line with LTC strategies which are generally centered on ultra-low NO_x emissions. In order to obtain NO_x – CH_4 and NO_x – CO trade-off, the effect of split injection strategy on natural gas/diesel dual-fuel combustion under similar engine load is investigated in the next section.

4.2. Split injection

In this section the effect of first pulse injection timing (28–55 °BTDC) with a fixed second pulse injection timing of 10 °BTDC and split injection ratio of 60% on combustion performance and emissions under 25% engine load is studied. Split injection ratio is defined as the mass ratio of diesel fuel injected in the first pulse divided by the total amount of the injected diesel fuel. The operating conditions for different split injection strategies are listed in Table 3.

4.2.1. Effect of split injection on combustion characteristics

Fig. 6 shows the experimental in-cylinder pressure and HRR of natural gas/diesel dual-fuel combustion of selected first injection timings under fixed split ratio of 60%, second injection timing of 10 °BTDC, and 25% engine load. Moreover, Fig. 7 displays a comparison between the experimental and numerical in-cylinder pressure and HRR profiles

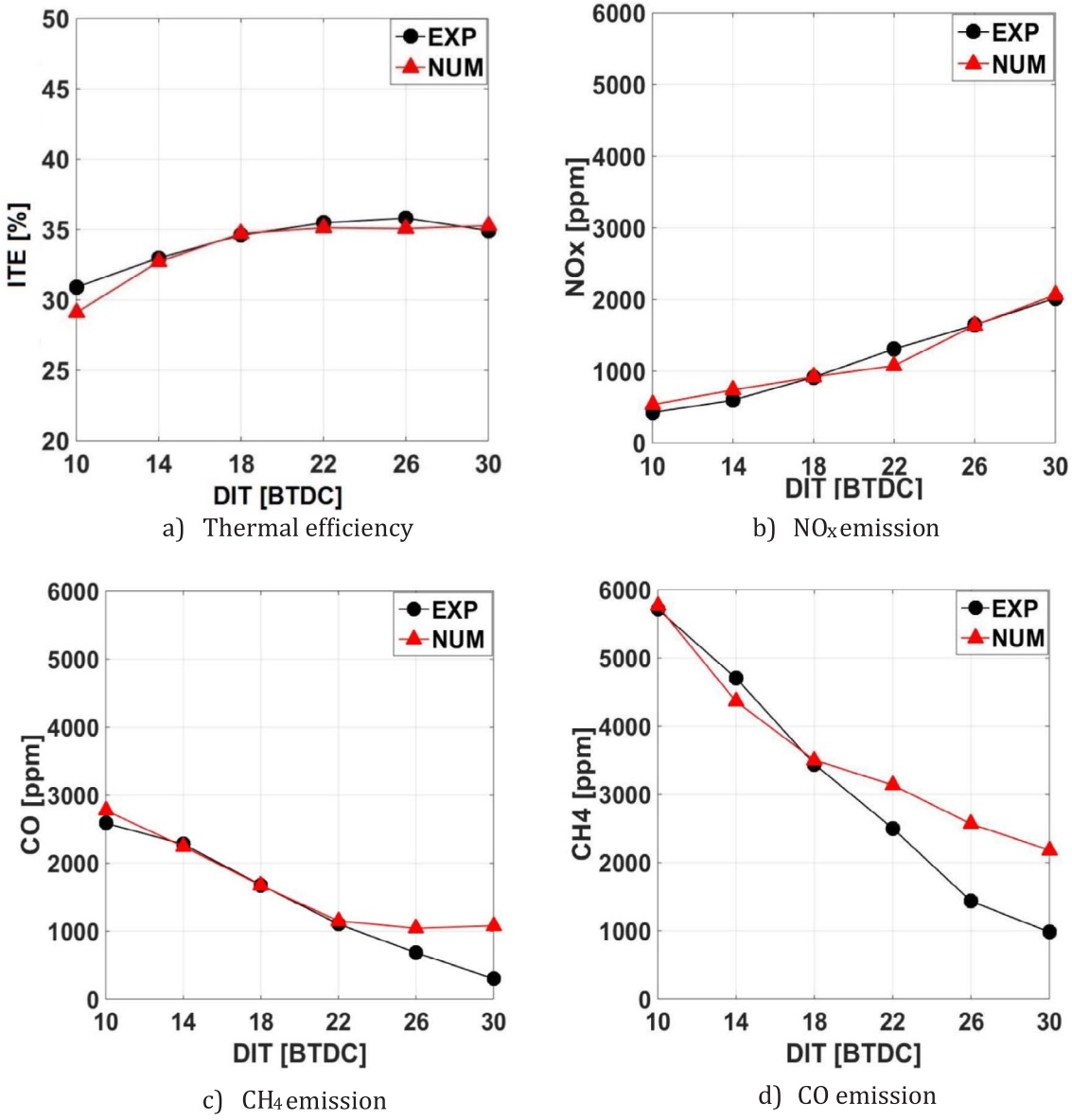

Fig. 5. Thermal efficiency and emissions of dual-fuel engine with single injection mode under 25% engine load.

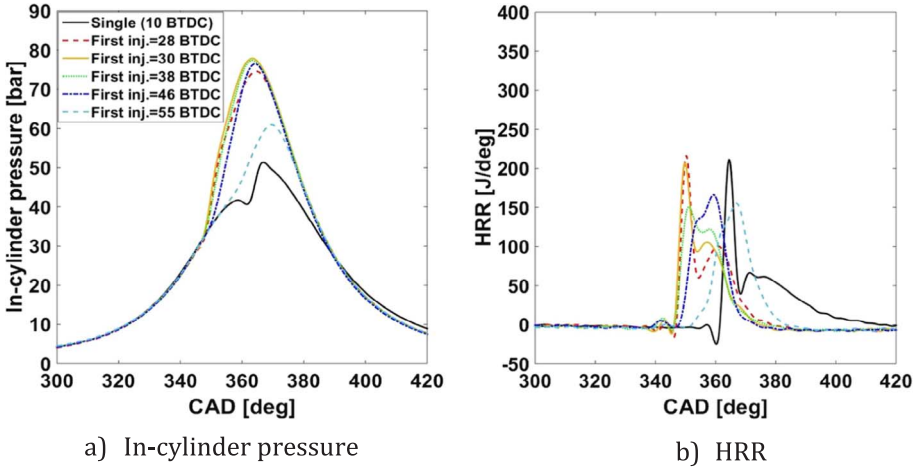

Fig. 6. Experimental in-cylinder pressure and HRR of dual-fuel mode with split injection under 25% engine load.

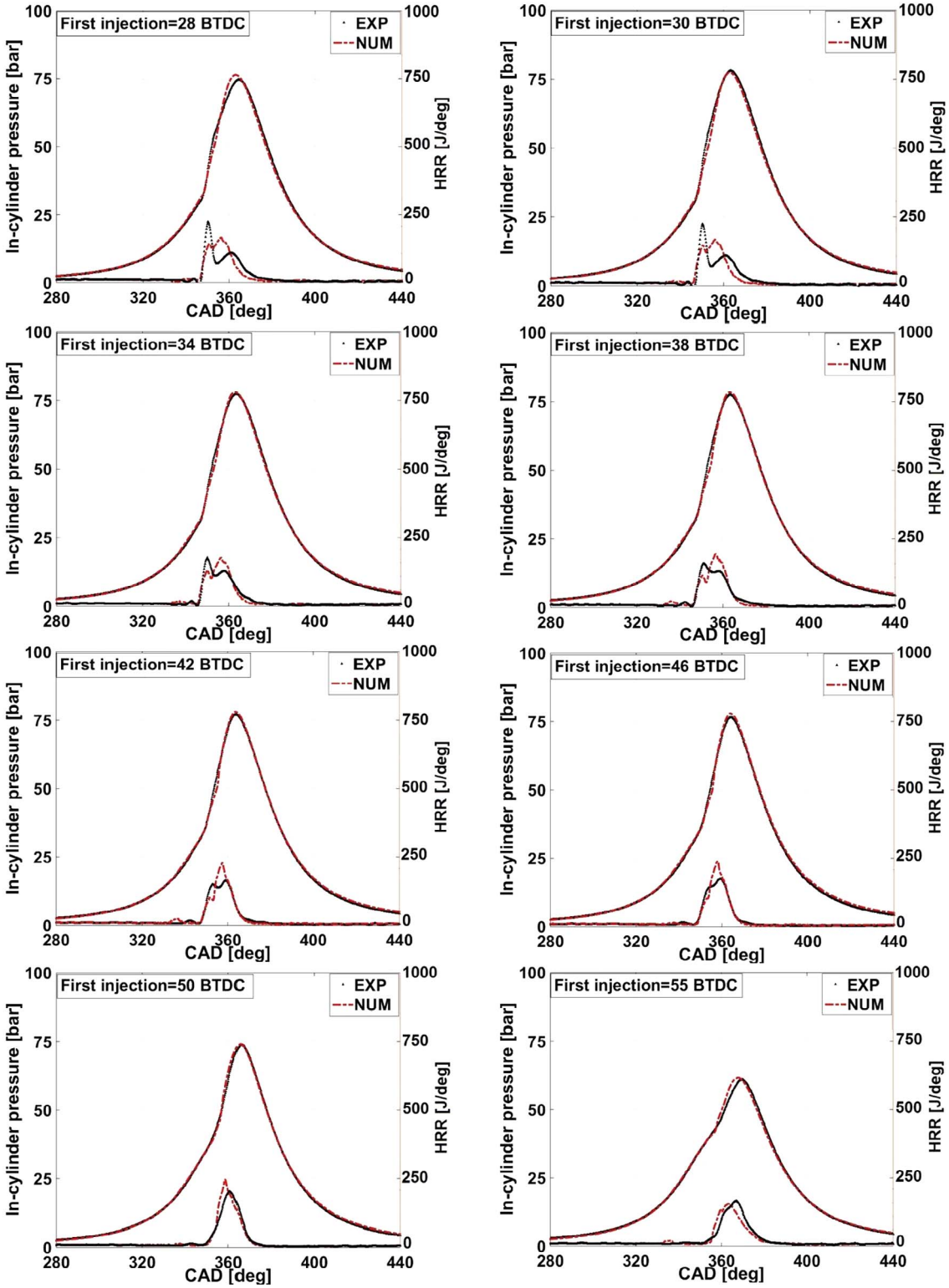

Fig. 7. Experimental and numerical comparison of in-cylinder pressure and HRR of dual-fuel combustion with split injection mode (different first injection timings and second injection timing of 10 °BTDC) under 25% engine load.

for different first injection timings (28–55 °BTDC) and second injection timing of 10 °BTDC. It can be seen, from Fig. 6a, that split injection mode considerably increases the in-cylinder peak pressure compared to that of single injection (10 °BTDC). Fig. 8 compares the in-cylinder temperature of different first injection timings with that of single injection (SOI = 10 °BTDC) at frame contours of 10 and 7 °BTDC. It can be observed that, compared to single injection mode, the heat release produced by first injection of diesel fuel considerably increases the in-cylinder charge temperature before the start of the second injection. The flame zone of the split injection mode is markedly higher than that of the single injection due to larger heat release produced during the first injection which promotes the combustion of the second one.

As shown in Figs. 6 and 7, when the first injection timing is close to the second injection timing (first injection timings of 28, 30, and 34

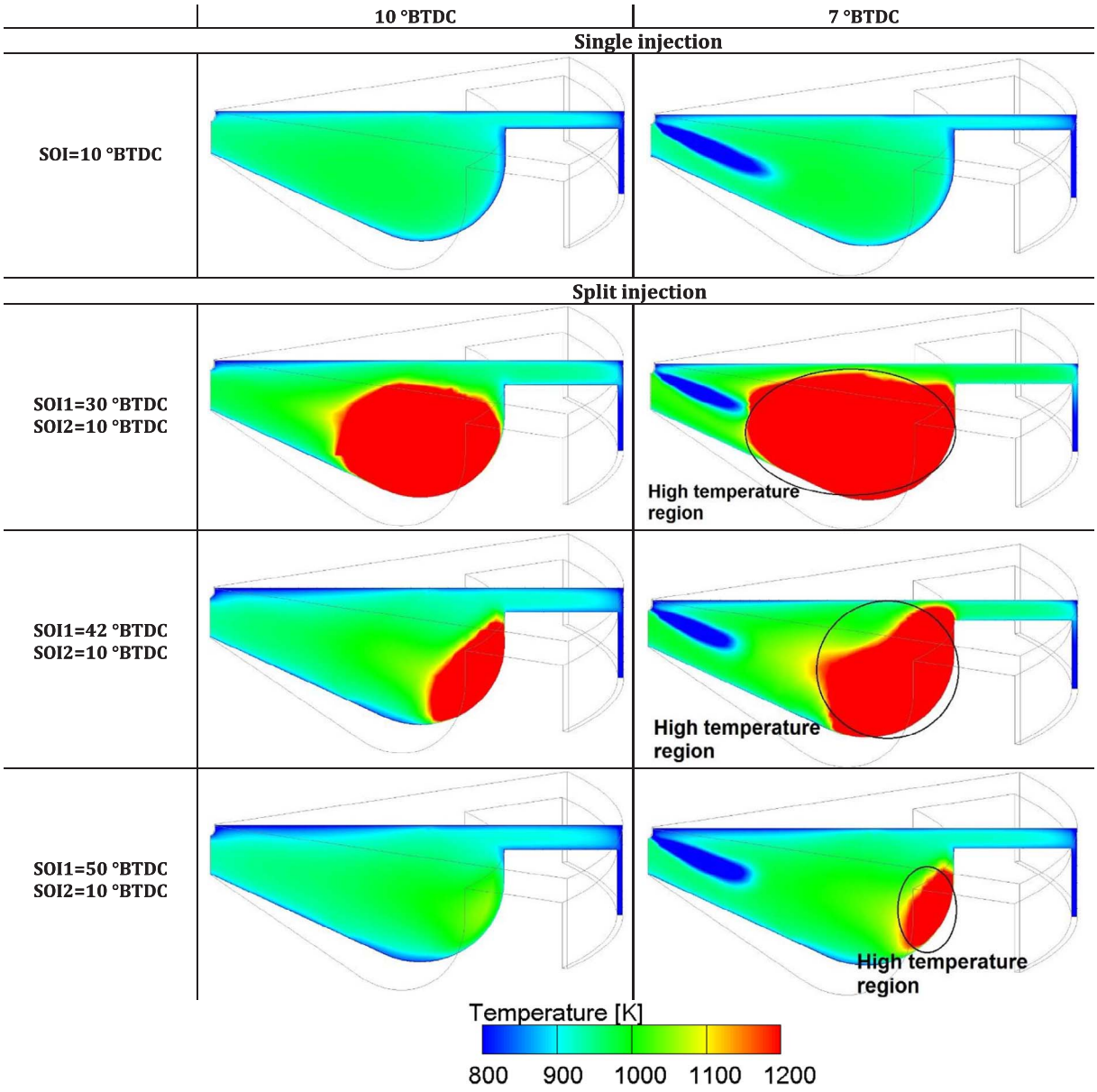

Fig. 8. In-cylinder temperature contours for single injection and split injection modes under 25% engine load at frame contours of 7 and 10 °BTDC.

°BTDC), the advancement of the first injection timing leads to increased peak in-cylinder pressure and HRR. This is mainly due to the advancement of combustion phasing toward TDC. Further advancing first injection timing (38–55 °BTDC) retards the SOC and shifts the combustion phasing away from TDC, leading to decreased peak in-cylinder pressure. Although the peak heat release rate happens slightly later for split injection than for single injection, the maximum pressure of split injection is higher than single injection when the first injection timing is 55 °BTDC. This is because of the significantly lower methane and CO emissions for split injection. As shown in Fig. 8, when the first injection timing is close to the second injection (i.e., SOI1 = 30 °BTDC), the second injected diesel fuel spray is close to the high temperature region resulting from the first injection of diesel fuel (flame kernels of the first injection pulse). Thus, the spray of the second injection and the initial stages of flame kernels of the first injection interact with each other, as indicated in Fig. 8 through the temperature distributions. Consequently, the effect of the first injection is more profound, which leads to increased ignition area of the in-cylinder mixture, earlier SOC (Fig. 9a) and combustion phasing, and increased in-cylinder peak pressure. Further advancing the first injection timing (38–55 °BTDC) weakens its influence on the combustion of the second injected diesel fuel. This is due to the fact that under advanced first injection timings (i.e. 42 and 50 °BTDC in Fig. 8), the second injected diesel fuel spray is located far away from the high temperature region resulted from the first injection of diesel fuel. Under this condition, very advanced first injection timing leads to longer ignition delay, which promotes air-fuel mixing and the formation of leaner air-natural gas and diesel fuel mixture. Thus, SOC (Fig. 9a) and combustion phasing are retarded which lead to reduced peak in-cylinder pressure.

In this study, the zero-crossing point of heat release curve is defined as SOC [46]. It can be seen from Fig. 9a that SOC advances firstly and then gradually delays, with advancing the first injection timing. When the first injection timing is close to the second injection timing (first injection timings of 28, 30, and 34 °BTDC), advancing the first injection timing makes the mixing of diesel and natural gas/air mixture start earlier and therefore advances SOC. Further advancing the first injection timing (38–50 °BTDC) results in lower in-cylinder thermal environment at the time of first injection, which leads to longer ignition delay and retarded SOC. This is effective for improving the mixing of natural gas-air and the diesel fuel injected by the first injection and

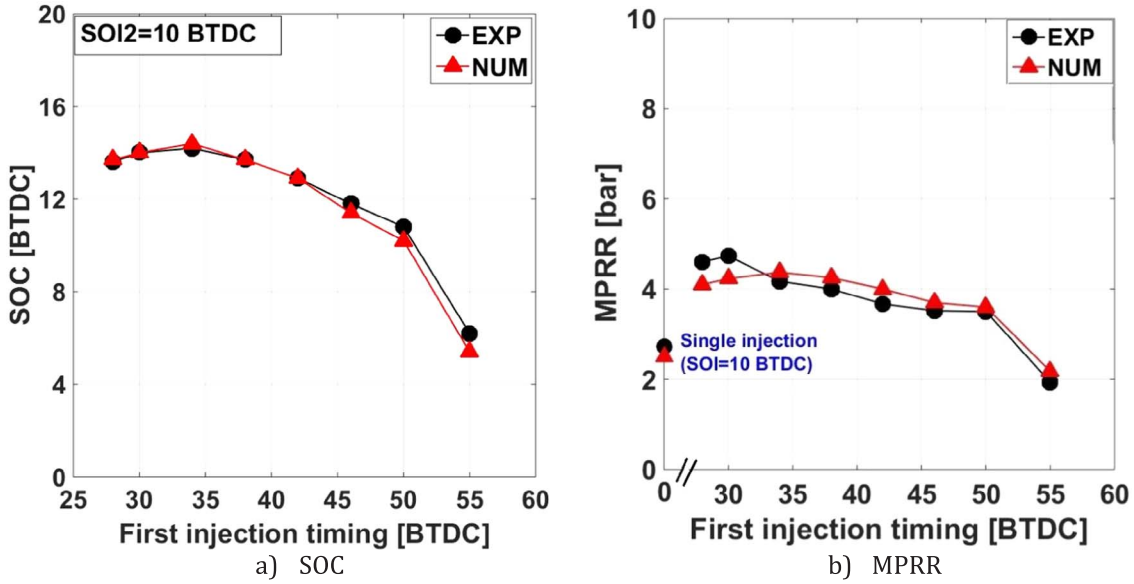

Fig. 9. Experimental and numerical comparison of SOC and MPRR of dual-fuel combustion with split injection mode under 25% engine load.

consequently the formation of leaner air-natural gas-diesel mixture. It also helps reduce methane and CO emissions and improve thermal efficiency. At very advanced first injection timing of 55 °BTDC, the premixed charge mixture (including the first injection of diesel fuel and natural gas-air) is too lean to be ignited in the compression stroke so that the ignition timing of the premixed charge is determined by the second injection of diesel fuel. In this case, the combustion starts very late (5.1 °BTDC) after the second injection of diesel fuel (Fig. 9a).

Fig. 9b shows the maximum pressure rise rate (MPRR) of single and split injection modes under 25% engine load. The MPRR is usually adopted as an index to describe the intensity of combustion roughness. Combustion noise is closely related to MPRR, which is a problem for highly premixed combustion like LTC. As shown in this figure, when the first injection timing is close to the second injection timing, the MPRR of split injection mode is much higher than that of single injection. However, further advancing first injection timing continuously decreases the MPRR. This is due to the fact that advancing first injection timings weakens the effect of split injected fuel on premixed charge combustion. It retards the SOC and reduces the MPRR. For very advanced first injection timing of 55 °BTDC, the MPRR decreases significantly and is lower than that of single injection. As mentioned earlier, the SOC is very retarded (4.6 °BTDC) and occurs after the second injection timing. In this case the second injection of diesel fuel controls the ignition and combustion rate of the in-cylinder mixture.

Fig. 10 presents the spatial distribution of OH radical mass fraction for single injection timing of 10 °BTDC and selected first injection timings of 30, 42, 50, and 55 °BTDC at different crank angles of 3, 6, 10, and 15 °after the start of combustion (ASOC). The contours plane is located at a vertical distance of 11 mm from the nozzle tip (top view). Moreover, Fig. 11 depicts the in-cylinder charge temperature for these selected first injection timings at 8 °ASOC (side view). It can be observed, from Fig. 10, that OH radical distribution is wider and more intense for the first injection timing of 30 °BTDC compared to single injection (10 °BTDC) and other first injection timings at initial stages of combustion (frame contours of 3 and 6 °ASOC). As shown in this figure, for this case, due to high temperature and pressure of premixed charge, the first injected diesel is directly ignited before the second injection timing. The second injected diesel fuel spray is close to the high temperature region resulting from the first injection of diesel fuel (flame kernels of the first injection pulse). Thus, the spray of the second injection and the initial stages of flame kernels of the first injection interact with each other and the second diesel injection undergoes auto-ignition instantly which leads to increased ignition area of the in-cylinder mixture in the directions of spray during the initial stages of combustion (Fig. 11). However, OH radical distribution for this case appeared throughout the injection zones and their sizes do not change significantly during the last stages of combustion (frame contours of 10 and 15 °ASOC). With advancing first injection timing (i.e., 42 and 50 °BTDC), the overall growth rate of OH radical becomes slower, its distribution is narrower, and the blue non-reactive zones are wider than those observed with a late first injection timing in the initial stages of combustion. However, they gradually continue to grow during last stages of combustion in the expansion stroke, indicating that a more premixed combustion takes place in these cases (Figs. 10 and 11). It increases heat release during the expansion stroke which results in increased thermal efficiency. It is notable that for these cases (i.e., SOI1 = 42 and 50 °BTDC), the OH radicals are detected in two zones at 10 °ASOC. The first zone is found near the wall region of piston bowl which corresponds to the high temperature fuel rich zones of first injected fuel and the second one is detected closer to the cylinder axis and nozzle tip which corresponds to the second diesel fuel injection (see Fig. 11). Moreover, for very advanced injection timing of 55 °BTDC, the OH distribution is similar to that of the single injection mode with lower OH intensity at initial stages of combustion (3 °ASOC). For this case, the premixed charge (air-natural gas-first injected diesel) is very lean and the second injection of diesel fuel mostly controls the ignition of the premixed charge. It can be seen that the OH radicals are detected very close to cylinder axis and nozzle tip and they barely grow during the late expansion stroke (Fig. 10). Moreover, the OH distribution is much narrower than that of the first injection timings of 30, 42, and 50 °BTDC, however, it is still wider than that of single injection (10 °BTDC).

4.2.2. *Effect of split injection on engine performance and emissions*

Fig. 12 shows the ITE of natural gas/diesel dual-fuel combustion under single injection timing of 10 °BTDC and different first injection timings at 25% load condition. As shown in this figure, a considerable improvement in ITE can be observed when using split injection strategy. The ITE of dual-fuel combustion with split injection mode is increased (on average) by 7% compared to that of single injection mode. Moreover, the highest thermal efficiency (38.04%) is obtained at the first injection timing of 50 °BTDC. It can be seen that the ITE continuously increases with advancing the first injection timing from 28 to 50 °BTDC. As shown in Figs. 10 and 11, with advancing the first

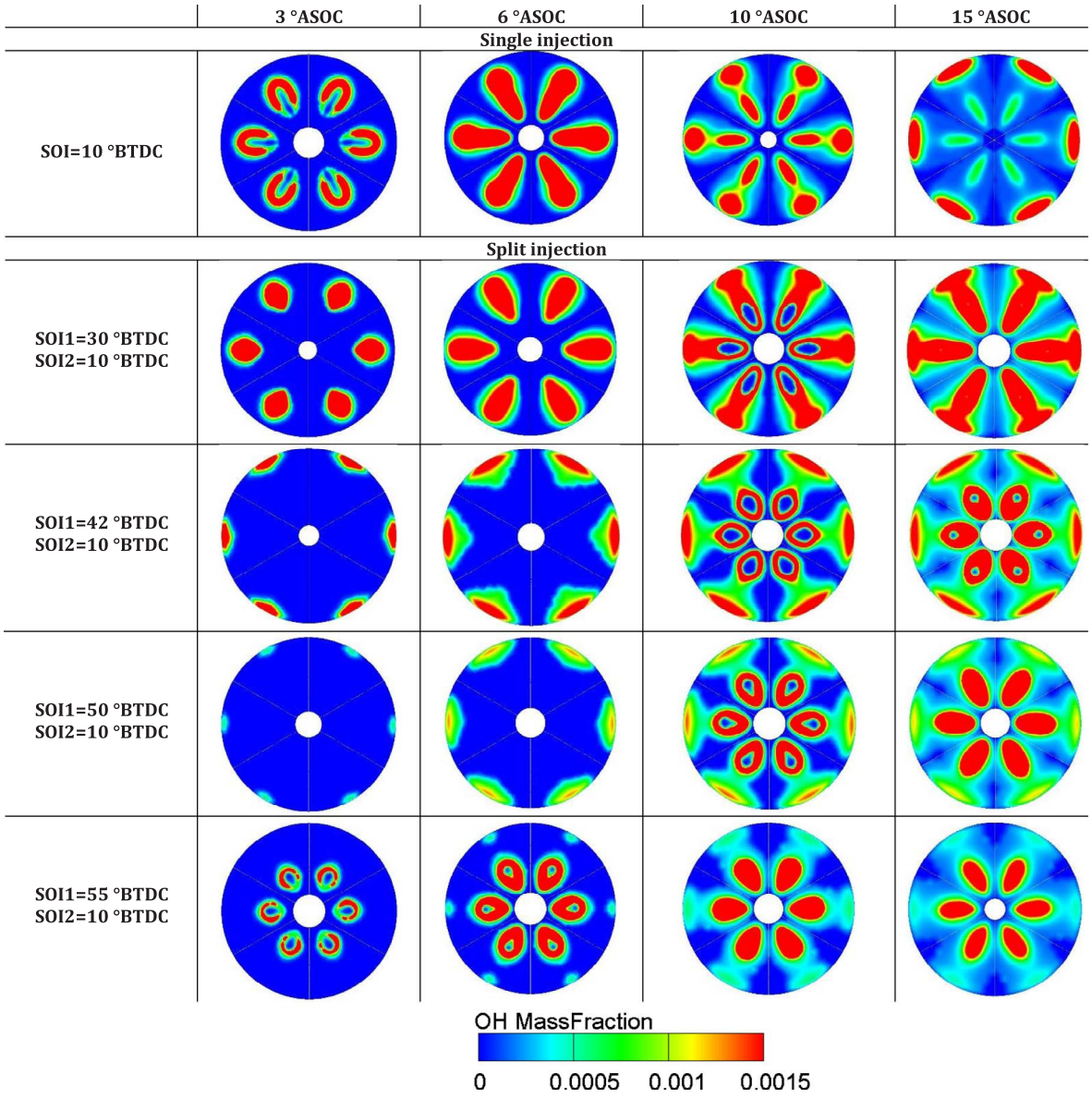

Fig. 10. Spatial contours of OH radical for selected single and split injection modes under 25% engine load.

injection timing, the premixed ignition of diesel-air-natural gas mixture provides a significant wide ignition source for natural gas, resulting in a faster combustion rate of natural gas-air mixture. The multipoint premixed combustion dominated by natural gas occurs quickly after the premixed combustion of pilot diesel fuel which results in improved premixed combustion of natural gas and more released heat during the premixed combustion stage. This late released heat positively affects the expansion pressure which leads to an increase in ITE. However, the ITE starts to drop for very advanced first injection timing of 55 ˚BTDC. This is due to the late start of combustion which causes combustion process to be shifted into the expansion stroke which results in lower in-cylinder pressure during the expansion stroke. This yields an increase in unburned methane and CO emissions (Fig. 13) which leads to a decrease in thermal efficiency.

Fig. 13a depicts the variation of NO_x emissions under different first injection timings and single injection timing of 10 ˚BTDC at 25% engine load. The formation of NO_x is related to combustion temperature and oxygen concentration. Higher in-cylinder charge temperature and oxygen concentration and longer reaction times result in more NO_x formation. It is observed that the experimental NO_x trend is well captured numerically. However, the model quantitatively over-predicts NO_x emissions. Moreover, it can be seen that a late first injection timing significantly increases NO_x emissions compared to that of single injection mode. This is because the first injected diesel is directly ignited due to high in-cylinder charge temperature. The second part of diesel fuel is injected during the combustion of the first injection, which leads to short interval time for sufficient air-fuel mixing. The local high combustion temperature regions are relatively wide (Fig. 14) which results in relatively higher NO_x emissions. Advancing first injection timing leads to leaner diesel and natural gas-air mixture formation. The ignition effect of the first injection of diesel fuel on the second injection weakens, resulting in delayed SOC. It prompts better air-fuel mixing which provides local lean and low combustion temperature regions, and thereby decreases largely NO_x formation. From Fig. 13a, it can be seen that, at first injection timing of 50 ˚BTDC, the level of NO_x emissions becomes similar to that of single injection mode (10 ˚BTDC).

The high level of unburned methane emissions of natural gas/diesel dual-fuel combustion at low load is caused by very lean premixed natural gas-air mixture and low chemical reactivity, low combustion rate due to extremely small amount of injected diesel fuel, and low in-cylinder charge temperature for premixed natural gas fuel oxidation [47,48]. Fig. 13b presents the unburned methane emissions for single

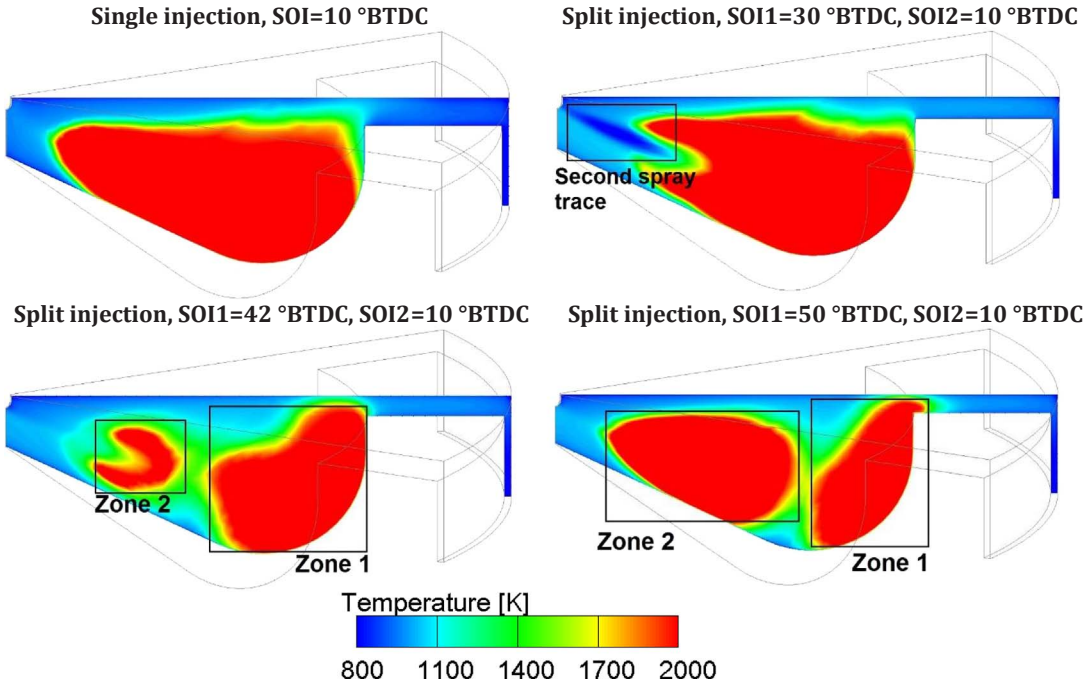

Fig. 11. In-cylinder temperature contours (at 8 °ASOC) of single and split injection modes under 25% engine load.

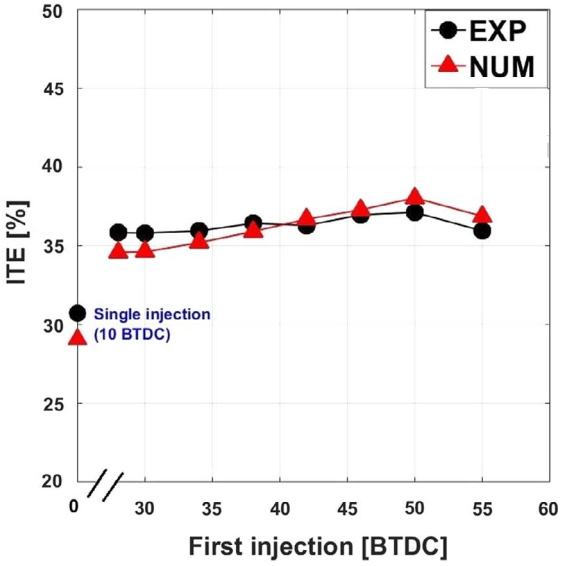

Fig. 12. Experimental and numerical comparison of ITE under 25% engine load.

injection timing of 10 °BTDC and different first injection timings under 25% engine load. The experimental results show that dual-fuel combustion with split injection mode significantly decreases unburned methane emissions compared to that of single injection mode (10 °BTDC). This trend is well reproduced by the CFD model. However, the numerical model over-predicts the unburned methane emissions under the examined first injection timings and misses the slight increase trend at first injection timings of 34–42 °BTDC. This might be due to the adopted reduced mechanism for natural gas/diesel dual-fuel combustion and also to the representation of diesel and natural gas by n-heptane and methane, respectively. Moreover, simulated methane emissions were predicted at EVO which may also contribute to the difference between the predicted and measured unburned methane emissions. It can be seen that the lowest methane emissions are achieved at very advanced first injection timing of 50 °BTDC. At this first injection timing, unburned methane emissions decrease by 60% compared to that of single injection. This is due to the improved premixed combustion and greater utilization of natural gas at earlier first injection timings. Further advancing first injection timing to 55 °BTDC increases the unburned methane emissions which are mainly due to a drop in combustion intensity during the expansion stroke.

The production of CO is mainly due to the incomplete combustion of fuels in the cylinder. Hence, CO is an intermediate product during the combustion process which can be formed in local oxygen deficit and low temperature regions. Excess air and combustion temperature greatly affect the oxidation reaction for converting CO to CO_2 [49]. Fig. 13c displays the CO emissions for single injection timing of 10 °BTDC and different first injection timings under 25% engine load. Due to the similar reason for the over-prediction of unburned methane emissions, the numerical model over-estimated the CO emissions under the examined first injection timings. However, its trend is well captured by the CFD model. It can be seen that compared to single injection mode, split injection considerably reduces the CO emissions. Compared to single injection, CO emissions are reduced by 63% at first injection timing of 50 °BTDC. Further advancing first injection timing (55 °BTDC) weakens the effect of first injected fuel on ignition and combustion intensity, and consequently leads to lower combustion temperature and increased CO emissions.

5. Conclusions

In this study, the effect of conventional single injection timing on the combustion and emissions characteristics of a natural gas/diesel dual-fuel combustion under low load conditions were investigated. Moreover, to achieve NO_x – CH_4 and NO_x – CO trade-off, the effect of split injection strategy under similar engine load was examined. The main conclusions of this study are summarized as follows:

- Natural gas/diesel dual-fuel engine at low loads experienced improved thermal efficiency and unburned methane and CO emissions at the expense of higher NO_x emissions when diesel injection is advanced from 10 to 30 °BTDC. Advancing single diesel injection timing from 10 to 30 °BTDC reduced unburned methane and CO emissions by 62% and 61% and increased thermal efficiency by 6%, but increased NO_x emissions by 74%.

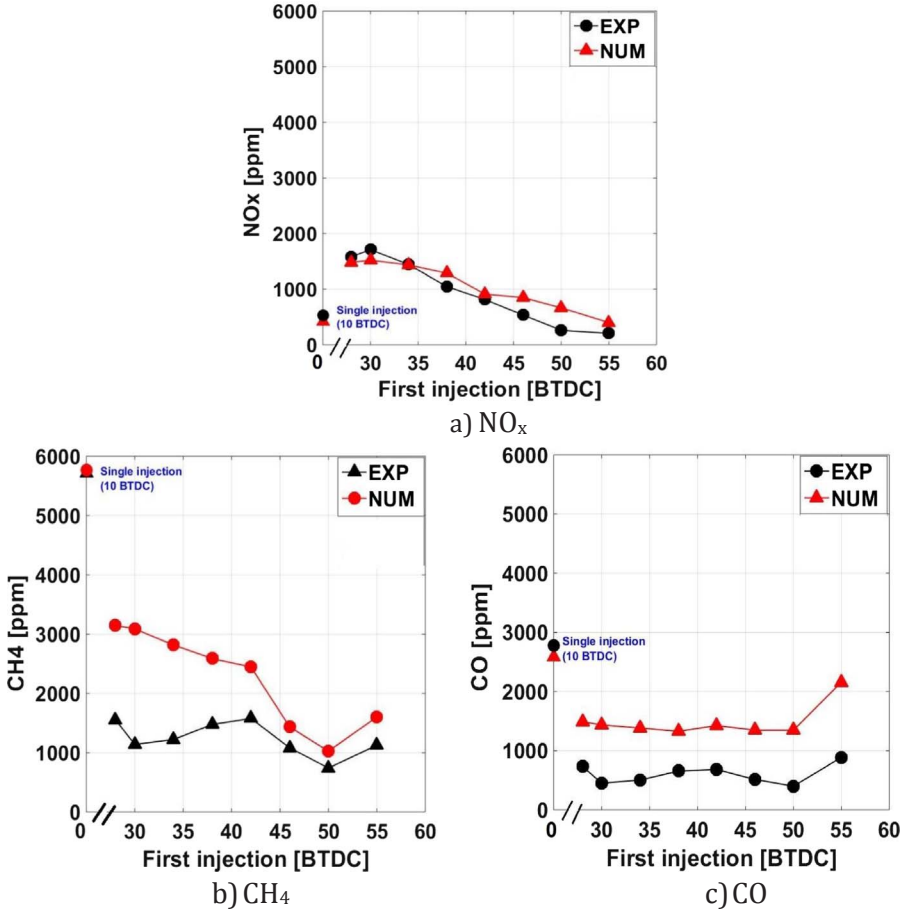

Fig. 13. Comparison between experimental and numerical emissions under 25% engine load.

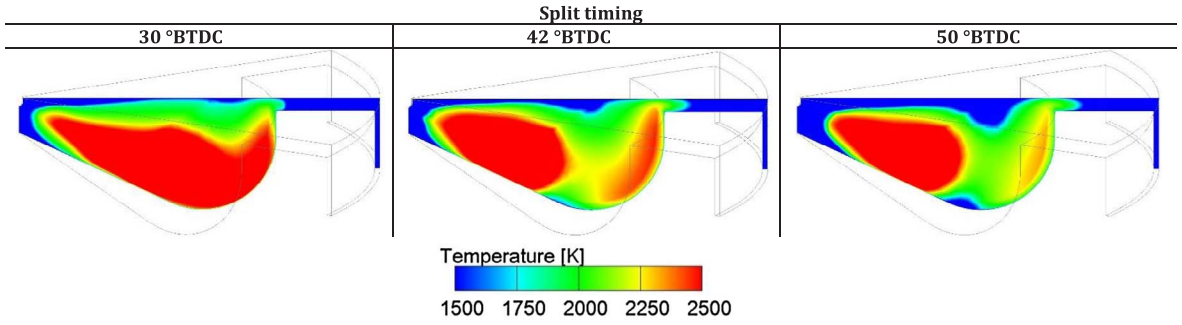

Fig. 14. In-cylinder temperature (at TDC) of selected first injection timings under 25% engine load.

- Split injection mode considerably increased the peak in-cylinder pressure compared to that of single injection (10 °BTDC). For late first injection timing, advancing the first injection timing led to increased peak in-cylinder pressure. Due to high temperature of premixed charge, first injected diesel directly ignited and the interaction between the spray of the second injection and the initial stages of flame kernels led to increased ignition area of the in-cylinder mixture. Further advancing the first injection timing weakened the influence of the first injection of diesel fuel combustion on the second injection combustion. Moreover, at very advanced first injection timing of 55 °BTDC, the ignition of premixed charge is mainly controlled by the second diesel fuel injection.
- For advanced first injection timings (38–50 °BTDC), the overall growth rate of OH radical became slower with a narrower distribution, and a wider blue non-reactive zones than those observed with a late first injection timing in the initial stages of combustion. However, they exhibited a gradual growth during the last stages of combustion in the expansion stroke, indicating that a more premixed combustion occurred in these cases. For first injection timings of 42 and 50 °BTDC, the OH radicals were detected in the two zones during the last stages of combustion. Moreover, for very advanced injection timing of 55 °BTDC, the OH distribution is similar to that of the single injection mode with lower OH intensity at initial stages of combustion.
- The ITE of dual-fuel combustion with split injection mode increased (on average) by 7% compared to that of single injection mode. ITE continuously increased with advancing first injection timing from 28 to 50 °BTDC and the highest thermal efficiency of 38.04% was achieved at first injection timing of 50 °BTDC. However, the ITE started dropping for very advanced injection timing of 55 °BTDC as

a result of late combustion phasing during the expansion stroke. Applying closely first injection timing significantly increased NO_x emissions compared to that of single injection mode. However, advancing first injection timing led to improved air-fuel mixing and lessened high combustion temperature regions, which consequently diminished NO_x formation. Moreover, the lowest methane and CO emissions were achieved at very advanced first injection timing of 50 °BTDC due to improved premixed combustion and greater utilization of natural gas at earlier first injection timings.

The trade-off between NO_x – CH_4 and NO_x – CO was accomplished with the application of split injection strategy. Compared to single injection, first injection timing of 50 °BTDC decreased unburned methane and CO emissions by, respectively, 60% and 63% and increased the thermal efficiency by 8.9%. However, NO_x emissions was maintained at the same level as that of single injection mode (10 °BTDC).

Acknowledgements

AVL Fire Software is provided by AVL Advanced Simulation Technologies. The financial support provided by the Natural Sciences and Engineering Research Council of Canada (NSERC) and the University of Manitoba (UMGF for Amin Yousefi) is gratefully appreciated. Funding for the experimental work was provided by Natural Resources Canada through the PERD Energy End Use (project 3B03.003), and National Research Council Canada through the internal Bioenergy Program.

References

[1] Qiu L, Cheng X, Liu B, Dong S, Bao Z. Partially premixed combustion based on different injection strategies in a light-duty diesel engine. Energy 2016;96:155–65. http://dx.doi.org/10.1016/j.energy.2015.12.052.
[2] Pedrozo VB, May I, Dalla Nora M, Cairns A, Zhao H. Experimental analysis of ethanol dual-fuel combustion in a heavy-duty diesel engine: an optimisation at low load. Appl Energy 2016;165:166–82. http://dx.doi.org/10.1016/j.apenergy.2015.12.052.
[3] Musculus MPB, Miles PC, Pickett LM. Conceptual models for partially premixed low-temperature diesel combustion. vol. 39. Elsevier Ltd; 2013. http://dx.doi.org/10.1016/j.pecs.2012.09.001.
[4] Yousefi A, Birouk M. Fuel suitability for homogeneous charge compression ignition combustion 2016;119:304–15.
[5] Jung D, Iida N. Closed-loop control of HCCI combustion for DME using external EGR and rebreathed EGR to reduce pressure-rise rate with combustion-phasing retard. Appl Energy 2015;138:315–30. http://dx.doi.org/10.1016/j.apenergy.2014.10.085.
[6] Bendu H, Murugan S. Homogeneous charge compression ignition (HCCI) combustion: mixture preparation and control strategies in diesel engines. Renewable Sustainable Energy Rev 2014;38:732–46. http://dx.doi.org/10.1016/j.rser.2014.07.019.
[7] Saxena S, Bedoya ID. Fundamental phenomena affecting low temperature combustion and HCCI engines, high load limits and strategies for extending these limits. Prog Energy Combust Sci 2013;39:457–88. http://dx.doi.org/10.1016/j.pecs.2013.05.002 Review.
[8] Yousefi A, Gharehghani A, Birouk M. Comparison study on combustion characteristics and emissions of a homogeneous charge compression ignition (HCCI) engine with and without pre-combustion chamber. Energy Convers Manag 2015;100:232–41. http://dx.doi.org/10.1016/j.enconman.2015.05.024.
[9] Sahoo BB, Sahoo N, Saha UK. Effect of engine parameters and type of gaseous fuel on the performance of dual-fuel gas diesel engines-A critical review. Renew Sustain Energy Rev 2009;13:1151–84. http://dx.doi.org/10.1016/j.rser.2008.08.003.
[10] Yousefi A, Birouk M. Investigation of natural gas energy fraction and injection timing on the performance and emissions of a dual-fuel engine with pre-combustion chamber under low engine load. Appl Energy 2017;189:492–505. http://dx.doi.org/10.1016/j.apenergy.2016.12.046.
[11] Yousefi A, Birouk M, Lawler B, Gharehghani A. Performance and emissions of a dual-fuel pilot diesel ignition engine operating on various premixed fuels. Energy Convers Manag 2015;106:322–36. http://dx.doi.org/10.1016/j.enconman.2015.09.056.
[12] Hosmath RS, Banapurmath NR, Khandal SV, Gaitonde VN, Basavarajappa YH, Yaliwal VS. Effect of compression ratio, CNG flow rate and injection timing on the performance of dual fuel engine operated on honge oil methyl ester (HOME) and compressed natural gas (CNG). Renew Energy 2016;93:579–90. http://dx.doi.org/10.1016/j.renene.2016.03.010.
[13] Carlucci AP, Laforgia D, Saracino R, Toto G. Combustion and emissions control in diesel-methane dual fuel engines: The effects of methane supply method combined with variable in-cylinder charge bulk motion. Energy Convers Manag 2011;52:3004–17. http://dx.doi.org/10.1016/j.enconman.2011.04.012.
[14] Yang B, Wang L, Ning L, Zeng K. Effects of pilot injection timing on the combustion noise and particle emissions of a diesel/natural gas dual-fuel engine at low load. Appl Therm Eng 2016;102:822–8. http://dx.doi.org/10.1016/j.applthermaleng.2016.03.126.
[15] Aksu C, Kawahara N, Tsuboi K, Kondo M, Tomita E. Extension of PREMIER combustion operation range using split micro pilot fuel injection in a dual fuel natural gas compression ignition engine: a performance-based and visual investigation. Fuel 2016;185:243–53. http://dx.doi.org/10.1016/j.fuel.2016.07.120.
[16] Yousefi A, Birouk M. An investigation of multi-injection strategies for a dual-fuel pilot diesel ignition engine at low load. J Energy Resour Technol 2016;139:12201. http://dx.doi.org/10.1115/1.4033707.
[17] Ryu K. Effects of pilot injection timing on the combustion and emissions characteristics in a diesel engine using biodiesel-CNG dual fuel. Appl Energy 2013;111:721–30. http://dx.doi.org/10.1016/j.apenergy.2013.05.046.
[18] Srinivasan KK, Krishnan SR. Cyclic combustion variations in dual fuel partially premixed pilot-ignited natural gas engines. J Energy Resour Technol 2014;136:1–10. http://dx.doi.org/10.1115/1.4024855.
[19] Xu M, Cheng W, Li Z, Zhang H, An T, Meng Z. Pre-injection strategy for pilot diesel compression ignition natural gas engine. Appl Energy 2016;179:1185–93. http://dx.doi.org/10.1016/j.apenergy.2016.07.024.
[20] Yang B, Xi C, Wei X, Zeng K, Lai MC. Parametric investigation of natural gas port injection and diesel pilot injection on the combustion and emissions of a turbocharged common rail dual-fuel engine at low load. Appl Energy 2015. http://dx.doi.org/10.1016/j.apenergy.2015.01.037.
[21] Papagiannakis RG, Rakopoulos CD, Hountalas DT, Rakopoulos DC. Emission characteristics of high speed, dual fuel, compression ignition engine operating in a wide range of natural gas/diesel fuel proportions. Fuel 2010. http://dx.doi.org/10.1016/j.fuel.2009.11.001.
[22] Papagiannakis RG, Hountalas DT. Combustion and exhaust emission characteristics of a dual fuel compression ignition engine operated with pilot diesel fuel and natural gas. Energy Convers Manag 2004;45:2971–87. http://dx.doi.org/10.1016/j.enconman.2004.01.013.
[23] Rao BN, Prem Kumar BS, Kumar Reddy KV. Effect of CNG flow rate on the performance and emissions of a Mullite-coated diesel engine under dual-fuel mode. Int J Ambient Energy 2015;750:1–8. http://dx.doi.org/10.1080/01430750.2015.1023835.
[24] Mikulski M, Wierzbicki S, Śmieja M, Matijošius J. Effect of CNG in a fuel dose on the combustion process of a compression-ignition engine. Transport 2015;30:162–71. http://dx.doi.org/10.3846/16484142.2015.1045938.
[25] Di Blasio G, Belgiorno G, Beatrice C, Fraioli V, Migliaccio M. Experimental evaluation of compression ratio influence on the performance of a dual-fuel methane-diesel light-duty engine. 2015;8. http://dx.doi.org/10.4271/2015-24-2460. 2015-24-2460.
[26] Bora BJ, Saha UK. Experimental evaluation of a rice bran biodiesel - biogas run dual fuel diesel engine at varying compression ratios. Renew Energy 2016;87:782–90. http://dx.doi.org/10.1016/j.renene.2015.11.002.
[27] Bora BJ, Saha UK. Optimisation of injection timing and compression ratio of a raw biogas powered dual fuel diesel engine. Appl Therm Eng 2016;92:111–21. http://dx.doi.org/10.1016/j.applthermaleng.2015.08.111.
[28] Yang B, Wei X, Xi C, Liu Y, Zeng K, Lai MC. Experimental study of the effects of natural gas injection timing on the combustion performance and emissions of a turbocharged common rail dual-fuel engine. Energy Convers Manag 2014. http://dx.doi.org/10.1016/j.enconman.2014.07.030.
[29] Abdelaal MM, Hegab AH. Combustion and emission characteristics of a natural gas-fueled diesel engine with EGR. Energy Convers Manag 2012;64:301–12. http://dx.doi.org/10.1016/j.enconman.2012.05.021.
[30] Hernandez JJ, Lapuerta M, Barba J. Separate effect of H2, CH4 and CO on diesel engine performance and emissions under partial diesel fuel replacement. Fuel 2016;165:173–84. http://dx.doi.org/10.1016/j.fuel.2015.10.054.
[31] Li W, Liu Z, Wang Z. Experimental and theoretical analysis of the combustion process at low loads of a diesel natural gas dual-fuel engine. Energy 2016;94:728–41. http://dx.doi.org/10.1016/j.energy.2015.11.052.
[32] Liu J, Yang F, Wang H, Ouyang M, Hao S. Effects of pilot fuel quantity on the emissions characteristics of a CNG/diesel dual fuel engine with optimized pilot injection timing. Appl Energy 2013;110:201–6. http://dx.doi.org/10.1016/j.apenergy.2013.03.024.
[33] Wang Z, Zhao Z, Wang D, Tan M, Han Y, Liu Z, et al. Impact of pilot diesel ignition mode on combustion and emissions characteristics of a diesel/natural gas dual fuel heavy-duty engine. Fuel 2016;167:248–56. http://dx.doi.org/10.1016/j.fuel.2015.11.077.
[34] Zhang Q, Li N, Li M. Combustion and emission characteristics of an electronically-controlled common-rail dual-fuel engine. J Energy Inst 2015:1–16. http://dx.doi.org/10.1016/j.joei.2015.03.012.
[35] Guo H, Neill WS, Liko B. An Experimental Investigation on the Combustion and Emissions Performance of a Natural Gas - Diesel Dual Fuel Engine at low and Medium Loads 2015;1:130–7. http://dx.doi.org/10.1115/ICEF2015-1041.
[36] Yousefi A, Birouk M, Guo H. An experimental and numerical study of the effect of diesel injection timing on natural gas/diesel dual-fuel combustion at low load. Fuel 2017;203:642–57. http://dx.doi.org/10.1016/j.fuel.2017.05.009.
[37] http://www.tfd.chalmers.se/~valeri/MECH.html n.d.
[38] Aggarwal SK, Awomolo O, Akber K. Ignition characteristics of heptane-hydrogen and heptane-methane fuel blends at elevated pressures. Int J Hydrogen Energy 2011;36:15392–402. http://dx.doi.org/10.1016/j.ijhydene.2011.08.065.
[39] Gmbh AVLL. AVL FIRE ® VERSION 2011 2011.

[40] Guo H, Liko B, Neil WS. Effect of Diesel Injection Split on Combustion and Emissions Performance of Natural Gas – Diesel Dual Fuel Engine at a Low Load Condition. Proc ASME, Intern Combust Engine Div Fall Tech Conf, ICEF2017-3584, October 15–18, 2017. Washington, USA: Seattle; 2017.
[41] Kong S, Marriott CD, Reitz RD. Modeling and experiments of hcci engine combustion using detailed chemical kinetics with multidimensional CFD. SAE Int J Engines 2001:1–2. http://dx.doi.org/10.4271/2001.
[42] Han Z, Reitz RD. Turbulence modeling of internal combustion engines using rng κ-ε models. Combust Sci Technol 1995;106:267–95. http://dx.doi.org/10.1080/00102209508907782.
[43] Module LM. AVL FIRE ® VERSION 2011 2011.
[44] Beale JC, Reitz RD. Modeling spray atomization with the kelvin-helmotz/rayleigh-taylor hybrid model. At Sprays 1999;9:623–50. http://dx.doi.org/10.1615/AtomizSpr.v9.i6.40.
[45] Butler TD, Cloutman LD, Dukowicz JK, Ramshaw JD. Multidimensional numerical simulation of reactive flow in internal combustion engines. 1981;7:293–315.
[46] G. Gao, F. Yang, M. Ouyang, C. Fang, SOC Detection of Diesel Engines Based on Online Estimation of Motored Pressure. Vol 1 Large Bore Engines; Adv Combust Emiss Control Syst Instrumentation, Control Hybrids 2013:V001T05A002. doi:10.1115/ICEF2013-19030.
[47] Zhang C, Song J. Experimental study of co-combustion ratio on fuel consumption and emissions of NG–diesel dual-fuel heavy-duty engine equipped with a common rail injection system. J Energy Inst 2015:1–8. http://dx.doi.org/10.1016/j.joei.2015.06.005.
[48] Liu J, Zhang X, Wang T, Zhang J, Wang H. Experimental and numerical study of the pollution formation in a diesel/CNG dual fuel engine. Fuel 2015;159:418–29. http://dx.doi.org/10.1016/j.fuel.2015.07.003.
[49] Huang H, Wang Q, Shi C, Liu Q, Zhou C. Comparative study of effects of pilot injection and fuel properties on low temperature combustion in diesel engine under a medium EGR rate. Appl Energy 2016;179:1194–208. http://dx.doi.org/10.1016/j.apenergy.2016.07.093.